Sparus Docking Station: A Current Aware Docking Station For a Non-holonomic AUV

Joan Esteba[1], Patryk Cieslak[1], Narcís Palomeras[1], and Pere Ridao[1]

[1]Universitat de Girona Parc Cientific i Tecnologic

May 10, 2023

Abstract

This paper presents the design and development of a funnel-shaped Sparus Docking Station (SDS) intended for the non-holonomic torpedo-shaped Sparus II Autonomous Underwater Vehicles (AUV). The SDS is equipped with sensors and batteries, allowing for a stand-alone long-term deployment of the AUV. An inverted Ultra Short BaseLine (USBL) system is used to locate the Docking Station (DS) as well as to provide long-term drift-less AUV navigation. The SDS is able to observe the ocean currents using a Doppler Velocity Log (DVL), being motorized to allow its self-alignment with the current. Moreover, a docking algorithm accounting for the current is used to guide the robot during the docking maneuver. The paper reports experimental results of the docking maneuver in sea trials.

Sparus Docking Station: A Current Aware Docking Station For a Non-holonomic AUV

Joan Esteba[*]

Computer Vision and Robotics Research Institute (VICOROB)

University of Girona

17003 Girona, Spain

`joan.esteba@udg.edu`

Patryk Cieślak

Computer Vision and Robotics Research Institute (VICOROB)

University of Girona

17003 Girona, Spain

`patryk.cieslak@udg.edu`

Narcís Palomeras

Computer Vision and Robotics Research Institute (VICOROB)

University of Girona

17003 Girona, Spain

`narcis.palomeras@udg.edu`

Pere Ridao

Computer Vision and Robotics Research Institute (VICOROB)

University of Girona

17003 Girona, Spain

`pere.ridao@udg.edu`

Abstract

This paper presents the design and development of a funnel-shaped Sparus Docking Station (SDS) intended for the non-holonomic torpedo-shaped Sparus II Autonomous Underwater Vehicles (AUV). The SDS is equipped with sensors and batteries, allowing for a stand-alone long-term deployment of the AUV. An inverted Ultra Short BaseLine (USBL) system is used to locate the Docking Station (DS) as well as to provide long-term drift-less AUV navigation. The SDS is able to observe the ocean currents using a Doppler Velocity Log (DVL), being motorized to allow its self-alignment with the current. Moreover, a docking algorithm accounting for the current is used to guide the robot during the docking maneuver. The paper reports experimental results of the docking maneuver in sea trials.

1   Introduction

During the last years, AUVs have been developed and improved to satisfy the needs for more complex and demanding tasks. This trend will surely rise, considering many fields that can benefit from this technology, including oil and gas industry, marine life monitoring and research, and renewable energy production (e.g., through offshore wind farms) (Page and Mahmoudian, 2020), (Whitcomb, 2000), (Nicholson and Healey, 2013). AUVs can provide new capabilities by performing tasks that are not achievable using Remotely Operated Vehicles (ROV)s, for example, an AUV can carry out large autonomous mapping or inspection missions (Carreras et al., 2018) that an ROV can not execute due to the limitations imposed by its tether. In addition, the use of AUVs can drastically reduce the high operational costs associated with the use of ROVs due to the reduced dependence on large support vessels, as well as the necessity of a smaller support crew. On the other hand, the fact that AUVs are not wired, limits their operating time to their battery capacity. The lack of a cable also drastically reduces the communication bandwidth. To perform missions that extend beyond their operating time, AUVs must be recovered to recharge or replace their batteries, and to download gathered data that can hardly be transmitted otherwise.

One solution already explored in the literature (Bellingham, 2016), that can be applied in places where it is necessary to conduct actions on a regular basis, is the development of an underwater support infrastructure, named DS, where the AUV can be docked to recharge its batteries and/or transmit collected data. A DS provides a resting place for an AUV, at which it can recharge, transfer the data collected during the mission, and wait for further instructions. It removes the need for retrieving the AUV after each task and, in consequence, reduces significantly the operational costs. All these concepts lie in the interest of the Long Term Deployment (LTD) research in underwater robotics. The main concept of the LTD is to allow the AUVs to remain at the operational site for a period ranging from days to months. This will allow the AUVs to perform new tasks, such as continuous surveillance or persistent inspection of underwater industrial infrastructures. This research provides both hardware and software innovations as well as field results to progress toward this goal. Nowadays, the LTD research is developed in multiple research projects (Pinto et al., 2021), (Universitat de Girona, b), (Universitat de Girona, a), (Mbari,), (Bluelogic,). One of them is the H2020 ATLANTIS project that aims to establish a pioneer pilot infrastructure capable of demonstrating key enabling robotic technologies for inspection and maintenance of offshore wind farms (Pinto et al., 2021). Within the scope of this project, both the aerial and underwater parts of a wind farm must be inspected autonomously, on a regular basis. To achieve the LTD proposed in the ATLANTIS project, a DS has been designed and built and an inspection-capable AUV has been adapted to this scenario. Next, an autonomous docking controller has been developed to follow the appropriate docking maneuver. For the controller to work, a localization system between the AUV and the DS has been implemented.

In this work, the authors present all the steps from hardware designs to field tests which resulted in a complete solution for the LTD of the Sparus II AUV. Starting from a state of the art of the experimental docking systems in literature, summarized in Section 2. Continuing with the presentation of the proposed LTD system for the Sparus II AUV presented in Section 3. Containing the hardware development, presenting the non-invasive LTD upgrade of the AUV in Section 3.1 and the main characteristics of the developed DS prototype in Section 3.2. And the software development, explaining the docking strategy in Section 3.3 and the navigation upgrade developed in the AUV in Section 3.4. And finalizing with the presentation of successful sea results in Section 4, developed in two different locations: in the Mediterranean sea (Spain) and in the Atlantic Ocean (Portugal).

2   State of the art

AUV docking stations have been under development since 1997 (Stokey et al., 1997) and multiple solutions have been already proposed in the literature, summarized in (Bellingham, 2016), (Yazdani et al., 2020), (Esteba et al., 2021). The challenges faced by the researchers developing DS systems include: detecting the DS, estimating a good localization between the DS and the vehicle, controlling the AUV till completing the

docking maneuver, latching the vehicle in the DS, and establishing a connection between the DS and the AUV to transmit data and/or power when possible. Considering these challenges, multiple designs, tailored to different applications and requirements, have been proposed.

Docking systems can be classified from different points of view being the most important one the capture mechanism and the perception systems used to detect the DS, as well as to estimate the relative position between the AUV and the DS. Regarding the capture mechanism, some of the most popular solutions are: pole docking (Singh et al., 2001), (Sarda and Dhanak, 2019), where the AUV catches a pole using a device designed for this purpose, usually installed on the front of the vehicle; landing docking (Kawasaki et al., 2004), where the AUV touches down over the DS; net docking (Kukulya et al., 2010), where the AUV collides with a trapping net; and funnel docking systems (McEwen et al., 2008), where the robot is introduced into a funnel-shaped structure. While some of these systems take into consideration the presence of ocean currents by construction (e.g., pole docking) most of these systems have a well-defined approaching direction that can be difficult to follow in presence of ocean currents, especially for nonholonomic vehicles. It is worth noting that controlling a nonholonomic vehicle to follow a given trajectory is more challenging, as it can not be actuated in all the degrees of freedom it can move.

The perception system, used to detect the DS as well as to estimate the relative position between the vehicle and the DS, is also an important element that clearly differentiates the application and requirements of one docking system with respect to another. Perception systems can be based on acoustics, mainly from position measurements (i.e., USBL) (McEwen et al., 2008); vision, with passive or active markers (Park et al., 2010); or a combination of several systems (Palomeras et al., 2018), (Fletcher et al., 2017).

Looking at all these solutions, it is clear that not all systems can be used in all situations. For instance, DS that use a pole or a net capturing mechanism can be useful to recover the vehicle but not to protect it for a large period of time. Also, systems that heavily rely on vision can not be used in places where water clarity can not be guaranteed.

After reviewing the main published systems, and considering applications that face long-term deployment requirements, the most popular capture mechanism for the application at hand is the funnel-shaped system that may provide data and power communication to the AUV as well as protection. Perception systems used for this typology of DS include position-based acoustics combined with passive or active landmarks that can be detected with a vision system. Regarding ocean currents, funnel-shaped systems are not the best suited because they enforce a very restricted approaching angle. However, two contributions, one in the form of modifications to the standard funnel-shaped DS hardware and the other in the control algorithm, are presented in this paper to overcome this problem.

Table 1 summarizes some of the most cited funnel-based systems that have been taken from the design phase to field experiments as well as their main characteristics. It compares the most determinant parameters from the DS systems:

1. **Localization system:** consists of the typology of the perception system used for localizing the DS from the AUV.

2. **Currents:** evaluates if the publication considers the ocean currents velocity vector.

3. **Comms and power**: considers if the published system presents a solution for connecting the AUV with the DS to transmit data (communication) and power.

4. **LTD or LaRS:** considers if the publication is developed as a Long Term Deployment system or a Launch and Recovery System.

5. **Controller:** considers the control system for the path-following of the AUV during the docking maneuver.

6. **Success rate:** evaluates the number of successful attempts against the total attempts published for each solution.

Authors	(Stokey et al., 2001)	(Feezor et al., 2001)	(Allen et al., 2006)	(McEwen et al., 2008)	(Park et al., 2009)	(Circle, 2012)	(Fletcher et al., 2017)	(Palomeras et al., 2018)
Localization system	Acoustics	Electro-magnetic	Acoustics	Acoustics	Vision	Acoustics	Acoustics and vision	Acoustics and vision
Currents	Yes	Yes	No	Yes	Yes	Yes	No	No
Comms and power	Yes	Yes	Yes	Yes	No	No	No	Comms only
LTD or LaRS	LTD	LaRS	LTD	LTD	LTD	LaRS	LaRS	LTD
Controller	Not published	PID	Not published	Cross-track	Custom	Pure pursuit	Pure pursuit	Pure pursuit
Success rate	Not published	5/8	17/29	4/4	Not published	7/11	6/25	12/15

Table 1: Summary of the most representative funnel-shaped DS systems published in the literature that achieved experimental results.

All the works presented in Table 1 use funnel-shaped DS that show experimental results. In (Stokey et al., 1997), a planar nose cone, to accommodate the vehicle, and four individual wide-band hydrophone signals, to estimate the DS location, were used. Field works are mentioned in the text but statistical results (related to the success rate) are not provided. In 2006, another experimental study was conducted (Allen et al., 2006) using a USBL as the main localization system. Experimental results provided in the article indicate 17 successful trials out of 29 attempts, which constitutes a 58% success rate. In 2008 (McEwen et al., 2008) designed and tested a funnel-shaped DS that was also using a USBL system for localization. Trials were carried out at 300 meters deep with an AUV that had to find the DS and then dock. The authors were able to perform four consecutive successful autonomous dockings. In 2012, the HYDRIOD group implemented an autonomous docking system also using a USBL system for localization purposes. The reported success rate for this system was 77% (Circle, 2012). In 2017, other sea experiments were performed (Fletcher et al., 2017), (Zhang et al., 2017), proving that funnel shape is a successful DS design. However, they do not take into consideration the effect of the currents in their trials. Finally, in 2018, a team from Universitat de Girona (UdG) developed another funnel-based solution that used a combination of acoustic ranges and active optical markers to localize the DS with respect to the AUV (Palomeras et al., 2018). Despite a success rate of 80%, the authors concluded that the system was not reliable in presence of ocean currents and that the optical part of the localization system was not suitable for high levels of water turbidity. Examining not only the systems mentioned above, but most of the articles on funnel-based docking published to date, the authors believe that it is possible to state that, to this day, there are still improvement needs in order to achieve a highly reliable solution for autonomous docking in real marine environments, especially when looking for long-term deployable systems in areas that may be affected by currents. Therefore, this article aims to provide novel solutions, both in the mechanical design and the localization and control software, that will help to achieve this goal.

3 Long Term Deployment system

This section describes the main developments of the different technologies that were needed to achieve the experimental results presented in this work. First, the AUV is presented as well as the hardware upgrades done to tackle the proposed LTD application. Second, the new prototype of a DS is presented. Third, the docking strategy, already explained in (Esteba et al., 2023), is presented. Finally, the navigation system implemented in the AUV to meet the necessary docking requirements is described.

3.1 Nonholonomic AUV: Sparus II

The Sparus II is an AUV developed primarily for seabed surveys and offshore structure inspection by the University of Girona, and recently commercialized by Iqua Robotics SL. (Carreras et al., 2013), (Carreras et al., 2018). It combines the classical concept of a torpedo-shaped vehicle with hovering capabilities (see Fig. 1). The main specifications and features of the Sparus II consist of:

- Length: 1.6 m.
- Hull diameter: 230 mm.
- Maximum width: 460 mm.
- Weight in air: 52 kg.
- Maximum depth: 200 m.
- Energy: 1.4 kWh Li-Ion battery.
- Endurance: from 8 to 10 hours.
- Maximum surge velocity: 3 kn.
- Propulsion system: 3 thrusters with magnetic coupling.
- Controllable Degree of Freedom (DoF): Surge, heave, and yaw.
- Building materials: Modular aluminum and acetal hull.
- Navigation sensors: DVL, Inertial Measurement Unit (IMU), pressure sensor, and Global Positioning System (GPS).
- Payload volume: 8 liters or 7 kg in air.
- Payload interface: Ethernet, RS-232, regulated 12 V and 24 V.
- Communications: WiFi, XBee, GSM/3G.

The shape of the AUV hull is optimized for navigation at medium/high velocities. The vehicle can be controlled in surge, heave, and yaw degrees of freedom independently by means of three thrusters (one vertical and two horizontal). It can reach a maximum velocity in surge of 3 kn. The vehicle is rated for up to 200 m depth. Its navigation suite includes an Inertial Measurement Unit (IMU), a Doppler Velocity Log (DVL), a Global Positioning System (GPS), a pressure sensor, and, optionally, a Ultra Short BaseLine (USBL). The latter can be used as a beacon to localize the AUV from the surface or, as inverted-USBL, to localize a target underwater, here the DS equipped with an acoustic beacon.

Its software architecture is based on Component Orientated Layer-based Architecture for Autonomy (COLA2) (Palomeras et al., 2012) which is utilizing the ROS open-source middleware (Quigley et al., 2009).
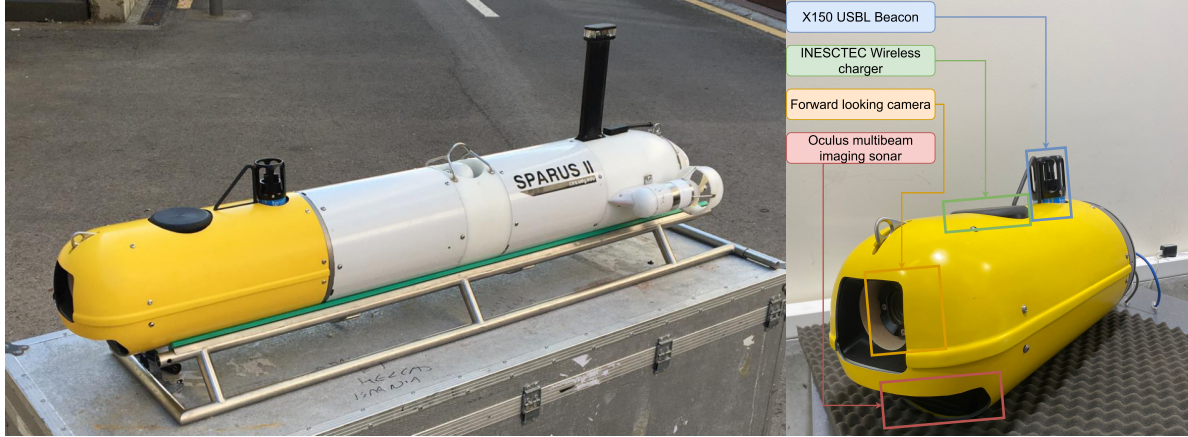
Figure 1: On the left, photography of the Sparus II AUV with the ATLANTIS project configuration. On the right, payload developed by Iqua Robotics that includes X150 USBL Beacon from Blueprint Subsea (Blueprint Design Engineering Ltd, b), Wireless charger prototype from INESCTEC, forward-looking camera from Iqua Robotics, and an Oculus M-Series from Blueprint Subsea (Blueprint Design Engineering Ltd, a).

The control system is divided into two parts: a guidance docking velocity controller based on the Managed Surge Controller (MSC) presented in section 3.3 and a low-level controller included within the COLA2.

To allow for the integration of mission-oriented equipment, the robot has a fully configurable payload area. In the ATLANTIS project, a new payload was designed and manufactured by Iqua Robotics (see Fig. 1). This payload was designed for mapping the seabed using a multibeam imaging sonar, allowing, also, for inductive charging, and including an USBL transceiver to locate the DS.

3.2 Sparus Docking Station

Given the torpedo shape of the non-holonomic AUV used, we opted for a funnel-shaped design, conceived as an evolution of the one presented in (Palomeras et al., 2018). The main difference with its predecessor is the capability to operate in low visibility environments using only acoustic feedback for its localization. Another significant advantage is the capability of self-alignment with the ocean currents to facilitate the docking. The SDS is made of two principal components, the tripod and the funnel, both of them described hereafter.

3.2.1 Tripod

The tripod is the base structure supporting the funnel. It is a tetrahedron frame made of 316 stainless steel pipes welded to laser-cut sheets. The tripod is designed to withstand the docking collision impacts transmitting the energy to the ground. The structure has two layers. The bottom one contains the pressure vessel (rated for 100-meter depth) with the batteries and the electronics. It is cabled to the SDS sensors, actuators, the inductive AUV charger, and the modems. The electronics (Fig. 5) include a Raspberry Pi 3 computer (Raspberry Pi,) and a microcontroller. The Raspberry Pi runs the Robot Operating System (ROS) (Quigley et al., 2009) middle-ware to manage the main system and the communication with the devices. The microcontroller manages the control of the motors and the power, implementing a sleep mode for battery consumption optimization. Finally, the cylinder hosts the battery (24 packs of NL2044 14.4V Lithium Ion Batteries). The top layer hosts the funnel rotation system. It consists of 4 elements: 1) the funnel orientation motor, 2) the linear actuator that brakes the rotation, 3) the gear system to transmit the torque, and 4) the two bearings of the funnel.
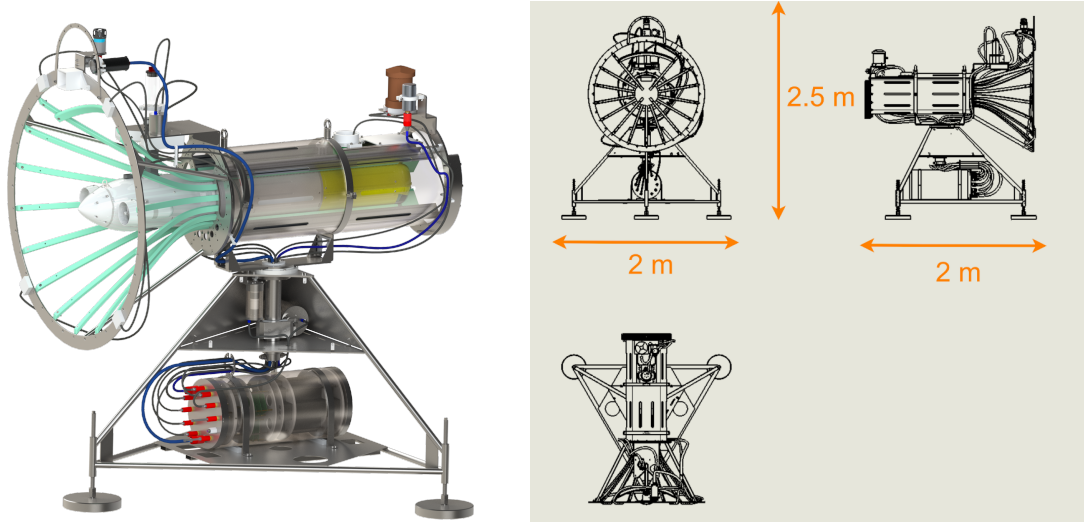
Figure 2: Conceptual representation of the Docking Station.

3.2.2 Funnel

The funnel is the assembly where the AUV docks, which includes (see Fig. 4) the following devices:

1. An USBL transponder/modem for localization and communication with the AUV (Blueprint Subsea Seatrack X110 (Blueprint Design Engineering Ltd, b)).

2. A camera to record the docking maneuvers.

3. A WiFi antenna for ultra-short-range high bandwidth communication. When docked, it allows the AUV to transmit the data logged during the mission to the DS.

4. A latching device, which clamps the AUV antenna to secure the position of the AUV inside the DS.

5. An inductive charger, developed by INESC TEC in the context of the ATLANTIS project.

6. An optical modem (10 MBs Luma X hydromea(Hydromea,)), for wireless high bandwidth communication with the AUV.

7. A DVL to measure the ocean current vector at the DS site (NavQuest LinkQuest 600 Micro (LinkQuest Inc,)) to align the DS.

The funnel entrance is manufactured using polyethylene M AST PE-1000 which, thanks to its properties, helps to absorb the collision energy of the docking maneuver, passively guiding the AUV to the DS. The tripod is designed to receive the collision impacts transmitting the energy to the ground. Finally, to lower the power required to rotate the funnel, an adjustable counterweight is used for its balance.

3.3 Docking controller

The MSC is a guidance controller for a nonholonomic AUV (Esteba et al., 2023) which drives the vehicle to the DS selecting the appropriate surge-velocity and heading set-points. It guides the robot along a line parallel to the main axis of the DS. The line offset depends on the ocean current, ensuring that the AUV nose targets the center of the funnel. When the robot nose touches the funnel, a surge/pitch controller is used to push ensuring a smooth entrance. Fig. 6 shows the main variables involved in the controller. The
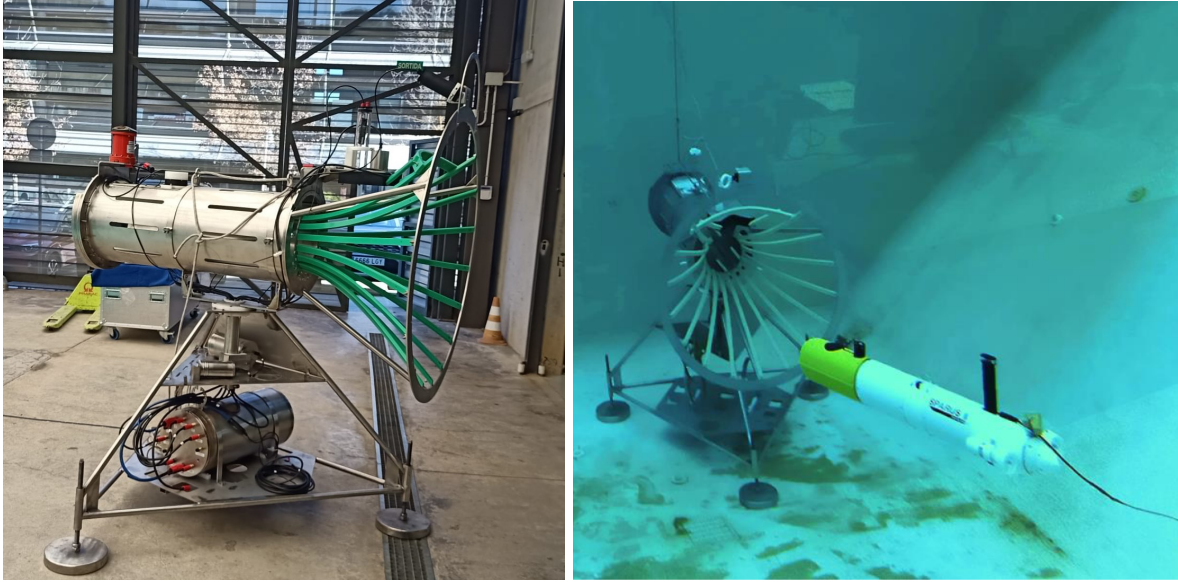
Figure 3: Docking Station photographies in the surface and into the CIRS (Centre d'Investigació en Robòtica Submarina) water tank with the Sparus II.
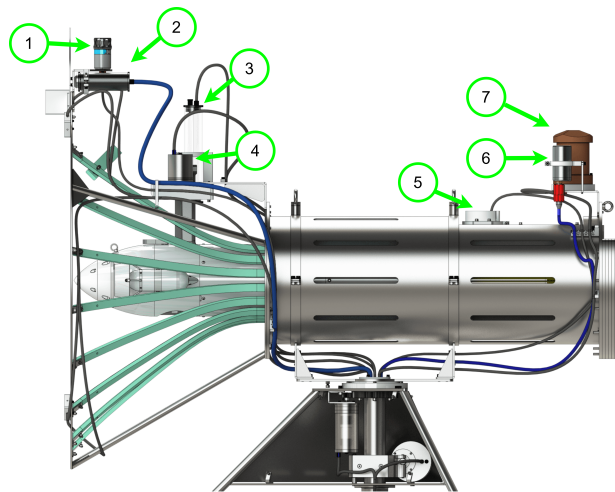

Figure 4: Sparus Docking Station funnel representation. 1) Acoustic modem from BluePrint Subsea, 2) camera, 3) WiFi antenna, 4) latching motor, 5) inductive charger from INESC TEC, 6) optical modem from Hydromea, 7) DVL from LinkQuest.
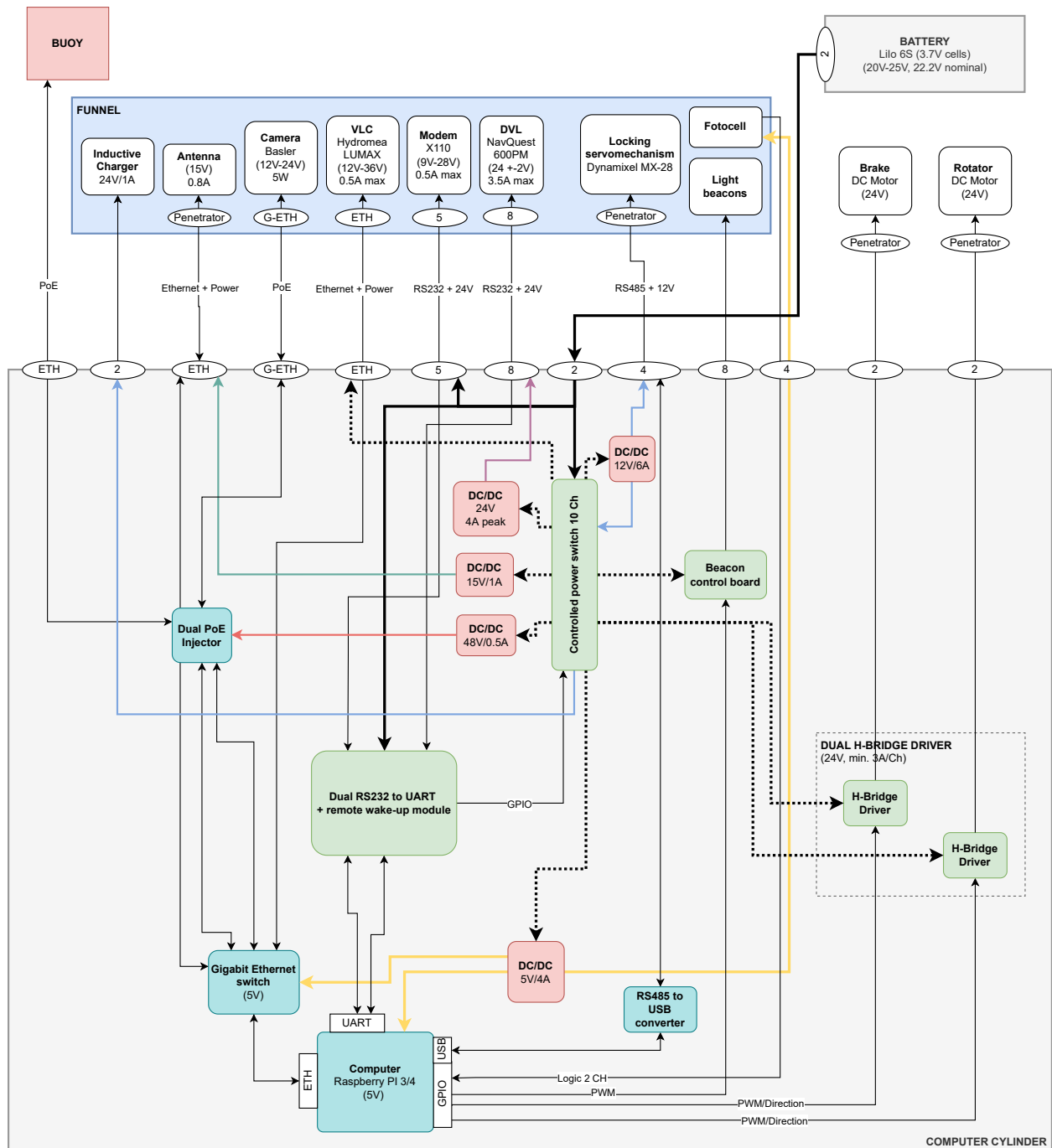
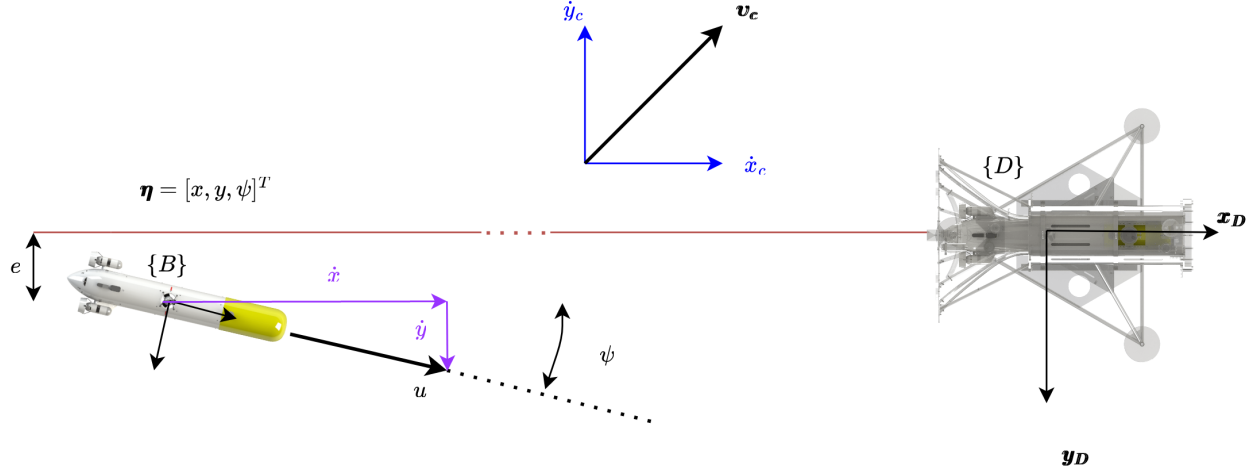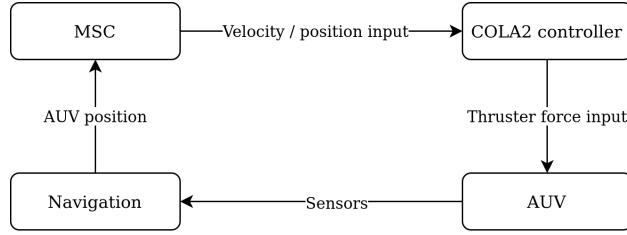Figure 5: Docking Station basic electrical schematic from the main cylinder.

Figure 6: MSC basic variables representation.

Figure 7: Conceptual representation of the Sparus II control system.

controller error dynamics are formulated as follows:

$$\dot{e} = u_d \ \sin(\psi) + \ \dot{y}_c, \tag{1}$$

where $\dot{e}$ is the time derivative of the cross-track error, u_d is the desired surge velocity, ψ is the heading of the AUV, and $\dot{y}_c$ is the projection of the ocean current velocity vector on the direction perpendicular to the DS main axis.

The controller law is defined as:

$$u_d = \frac{\dot{x}_{ss}}{\cos(\psi)} + c, \ c = -k_1 \ \text{atan}(k_2 \ e) \ \text{sign}(\psi) \tag{2}$$

$$\psi_d = \psi_c - \text{atan}\left(\ \frac{e}{\Delta}\right), \tag{3}$$

where $\dot{x}_{ss}$ and $\dot{y}_{ss}$ are the robot velocities with respect to water in the steady state (when the cross-track error vanishes to zero); k_1, k_2, and Δ are adjustable gains, e is the cross-track error, and ψ_c is a crab angle.

More details about the controller can be found in (Esteba et al., 2023), where its exponential stability is shown together with an exhaustive set of simulated results. The MSC was integrated into the vehicle's COLA2 (Palomeras et al., 2012) software architecture, acting as a guidance controller and issuing set-points to the velocity and heading vehicle controllers (see Fig. 7).

Once the AUV impacts the DS a constant surge velocity and a small pitch correction, are applied to achieve and smooth entrance. The pitch correction is achieved using the vertical thruster of the Sparus II AUV, taking advantage of the fact that the vehicle is touching with its nose the DS.

3.4 Inverted USBL navigation

In order to locate the DS, the AUV is equipped with an inverted USBL system, where the transceiver is mounted on the robot payload while the transponder is placed in the DS. To this aim, an Extended Kalman Filter (EKF) navigation method has been employed which fuses sensor data from a DVL, an Attitude and Heading Reference System (AHRS), a GPS, a depth sensor, and an USBL.
Following Fig. 8, let $\boldsymbol{\eta_1} = [x\ y\ z]^T$ be the robot position in the NED $N{-}frame$ and $\boldsymbol{\nu_1} = [u\ v\ w]^T$ its linear velocity vector referenced to the body fixed $B{-}frame$, the robot state vector has been defined defined as:

$$x_k = \begin{bmatrix} \eta_1 \\ \nu_1 \end{bmatrix} \tag{4}$$

Then, a constant velocity model with attitude input and acceleration noise is used as the motion model:

$$\bar{x}_k = f\left(x_{k-1}, u_k, w_k\right) = \begin{bmatrix} \eta_{1_{k-1}} + {}^{N}R_B(u_k + w_{\eta_{2_k}})\left(\nu_{k-1}\Delta t + w_{\dot{\nu}_{1_k}}\frac{\Delta t^2}{2}\right) \\ \nu_{k-1} + w_{\dot{\nu}_{1_k}}\Delta t \end{bmatrix} \tag{5}$$

where $\boldsymbol{u_k} = [\phi\ \theta\ \psi]^T$ is the robot attitude measured with the AHRS, and $\boldsymbol{w_k} = [\boldsymbol{w_{\eta_{2_k}}^T}\ \boldsymbol{w_{\dot{\nu}_k}^T}]^T$ is the motion model noise, composed of the AHRS noise $\boldsymbol{w_{\eta_{2_k}}} = [w_\phi\ w_\theta\ w_\psi]^T$ and the acceleration noise $\boldsymbol{w_{\dot{\nu}_k}} = [w_{\dot{u}}\ w_{\dot{v}}\ w_{\dot{w}}]^T$. The filter is updated with the observations from the navigation sensors. The DVL, the AHRS, the GPS, and the depth sensor provide linear observations of components of the state vector:

$$z_k = H_k \cdot x_k + v_k \tag{6}$$

each one having its corresponding observation vector, matrix, and noise:

- **DVL**: Provides the robot velocity in the $B{-}frame$.

$$z_{DVL} = \begin{bmatrix} z_u & z_v & z_w \end{bmatrix}^T \quad, \quad v_{DVL} = \mathcal{N}(0, R_{DVL})$$
$$z_{DVL} = H_k \cdot x_k + v_{DVL} \Rightarrow H_k = \begin{bmatrix} 0_{3\times3} & I_{3\times3} \end{bmatrix}$$

- **GPS**: Provides the robot position in the $N{-}frame$.

$$z_{GPS} = \begin{bmatrix} z_x & z_y \end{bmatrix}^T \quad, \quad v_{GPS} = \mathcal{N}(0, R_{GPS})$$
$$z_{GPS} = H_k \cdot x_k + v_{GPS} \Rightarrow H_k = \begin{bmatrix} I_{2\times2} & 0_{2\times4} \end{bmatrix}$$

- **Depth**: Provides the robot depth in the $N{-}frame$.

$$v_{depth} = \mathcal{N}(0, \sigma_{depth}^2)$$
$$z_{depth} = H_k \cdot x_k + v_{depth} \Rightarrow H_k = \begin{bmatrix} 0_{1\times2} & 1 & 0_{1\times3} \end{bmatrix}$$

Regarding the USBL observation $\boldsymbol{z_{USBL}} = [z_x\ z_y\ z_z]^T$, the non-linear USBL observation equation is given by:

$$\begin{aligned} z_{USBL} &= h_{USBL}(x_k, v_k) \\ &= F_1^T\left(\left[(\ominus^B x_U) \ominus (F_1\eta_1 + F_2(\eta_2 + v_{AHRS}))\right] \oplus {}^N x_D\right) + v_{USBL} \end{aligned} \tag{7}$$

where $\boldsymbol{F_1} = [\boldsymbol{I_{3\times3}\ 0_{3\times3}}]^T$ and $\boldsymbol{F_2} = [\boldsymbol{0_{3\times3}\ I_{3\times3}}]^T$ are projection matrices, $\boldsymbol{\eta_1}$ is the robot position within the state vector, $\boldsymbol{u_k} = \boldsymbol{\eta_2} = [\phi\ \theta\ \psi]^T$ is the robot attitude taken from the AHRS, ${}^{N}\boldsymbol{x_D}$ is the docking station pose in the $N{-}frame$ and ${}^{B}\boldsymbol{x_U}$ is the pose of the USBL transponder in the $B{-}frame$ (both of them
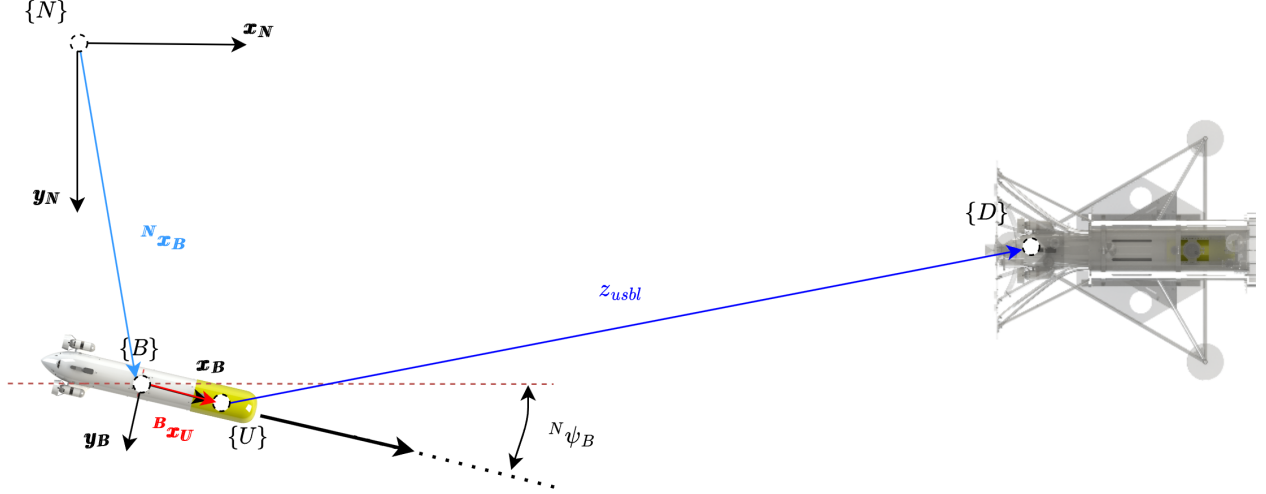
Figure 8: Reference systems used for the navigation.

constant and known a priori), while $v_k = [v_{USBL}^T \; v_{AHRS}^T]^T = \mathcal{N}(0, R_k)$ is the observation noise. Then, the observation Jacobians are given by:

$$
\begin{aligned}
H_k &= \frac{\partial h_{USBL}(x_k, v_k)}{\partial x_k} = \frac{\partial h_{USBL}(\eta_1, \eta_2, v_k)}{\partial [\eta_1 \; \nu_1]} = \begin{bmatrix} F_1^T J_{1\oplus} J_{2\ominus} F_1 & 0_{3\times3} \end{bmatrix} \\
V_k &= \frac{\partial h_{USBL}(x_k, v_k)}{\partial v_k} = \frac{\partial h_{USBL}(x_k, v_{USBL}, v_{AHRS})}{\partial [v_{USBL} \; v_{AHRS}]} = \begin{bmatrix} I_{3\times3} & F_1^T J_{1\oplus} J_{2\ominus} F_2 \end{bmatrix}
\end{aligned}
\tag{8}
$$

where $J_{1\oplus}$ and $J_{2\ominus}$ are the Jacobians of the 6 DoF compounding operation (Smith et al., 1990). Finally, is worth noting that the observations update the filter only if they satisfy an individual compatibility Chi-Square test, at a certain confidence level, to avoid the adverse effect of the outliers.

4   Results

This section reports the results of the experimental validation of the proposed system. First, the experiment conceived for the validation is described in section 4.1. Next, the selected experimental sites are presented followed by the results (sections 4.3 and 4.4).

4.1   Validation Experiment

The validation experiment was conceived to emulate a typical survey during a LTD mission. The Sparus II AUV started docked at the DS (located at a priory known pose), then undocked, executed a survey, and docked again autonomously as shown in Fig. 9. Different surveys, of different duration, were tested in order to check the robot's capability to dock after a mission, the longest one reaching 90 min of duration and completing a successful dock. To evaluate the repeatability of the system, most of the surveys were reduced to a minimum duration. At the end of the survey (Fig. 10), the robot executed a docking maneuver. First, the robot navigated towards a home position (1) in front of the DS, receiving updates in position from the USBL (2), then it followed a straight line (3) towards the funnel entrance. As explained in Section 3.3, this line might be slightly misaligned with the DS axis, to account for the ocean current. An inverted USBL navigation method (Section 3.4) was used during the whole maneuver to cancel the drift, accumulated during the survey, of the DVL-based navigation (4). When the robot touched the funnel of the docking station (5) a
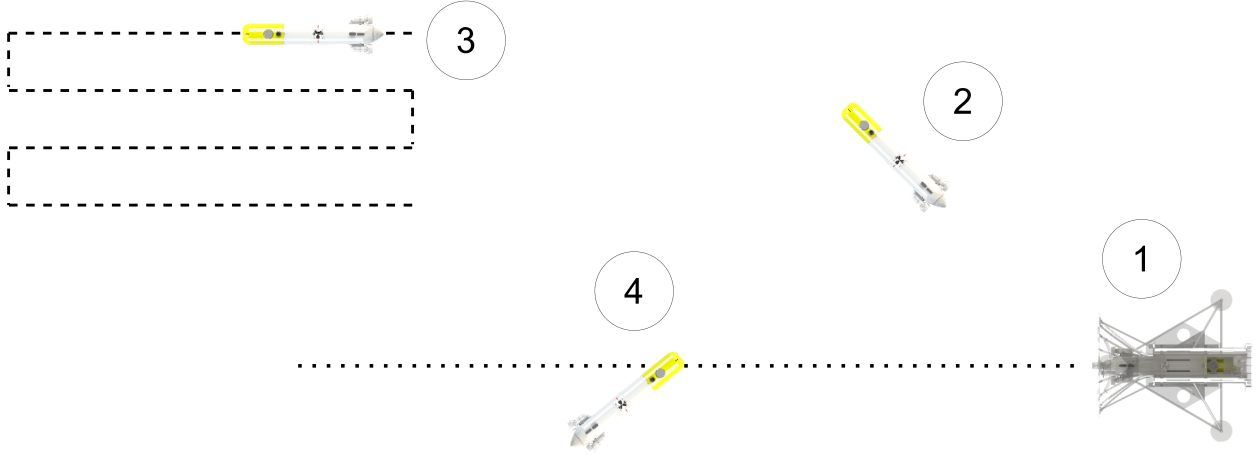
Figure 9: Experimental concept developed. 1) the Sparus II is inside the DS, 2) the Sparus II undocks and 3) performs the survey, 4) the docking maneuver is developed.

constant surge velocity and a small pitch correction, were applied to achieve and smooth entrance, completing the docking.

4.2 Experimental Setup

To test the experiment described above, the DS system was deployed in the calmed waters of the harbour of Sant Feliu (Girona, Spain), at 8 meters depth (Fig. 11, Fig. 12, and Fig. 13). Although the DS may self-orient according to the currents it measures, the absence of relevant currents in the harbour made us to adjust the DS heading manually (to maximise the maneuvering space) keeping it constant during the experiments. Therefore, the controller parameters were set as follows: $\psi_c = 0$; as reported in (Esteba et al., 2023) the gains were set as $k_1 = 0.4456\ m/s$, $k_2 = 1\ m^{-1}$, and $k_\Delta = 6\ m$. Finally, the desired docking velocity was set as $\dot{x}_{ss} = 0.3\ m/s$, to avoid strong collisions between the AUV and the DS. The controller was executed at a frequency of 100 Hz, with a navigation frequency of navigation of 15 Hz and including USBL fixes approximately every 2 seconds.

A second field deployment took place in the ATLANTIS Test Centre (INESC TEC,) (Fig.14), in Viana do Castelo (Porto, Portugal), at 8 meters depth with tides up to 2 meters. The DS location is shown in Fig.15. The test center is placed in the harbour, next to the mouth of the river Lima. There, the underwater visibility is very low as shown in Fig. 15 and Fig. 16, clearly justifying our docking strategy based only on acoustic sensor feedback. Again, the harbor protection made the current negligible.

4.3 Results in Sant Feliu

The validation began with several engineering tests to adjust the covariance matrices of the navigation sensors to achieve the required navigation accuracy. A batch of ten tests was performed first, achieving eight successful docking maneuvers and two failures. Fig. 17a shows the time evolution of the cross-tracking error of a representative successful test. It can be appreciated that at time -40 seconds an USBL fix (red line) arrives, updating the robot position estimate and, consequently, growing the cross-track error around 3 meters. This update is mostly attributed to the accumulated navigation drift. As expected, the MSC controller reacts, driving the robot in a direction minimizing the error, and successfully docking the vehicle. The MSC output variables, the heading, and the surge velocity are shown in Fig. 17. The heading is shown in Fig. 17b, where can be appreciated the reaction to the cross-track error, turning the robot towards the

Figure 10: Navigation of one autonomous docking example. 1) The Sparus II receives the command to start the docking maneuver, 2) the USBL applies an update to the Sparus II position, 3) the MSC controller starts, 4) while the AUV gets closer to the DS it's position is updated and the MSC has to react, 5) the AUV successfully docks.
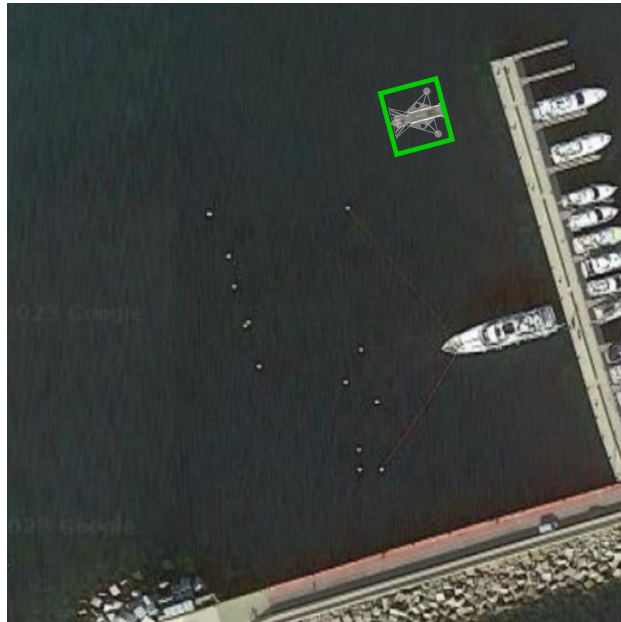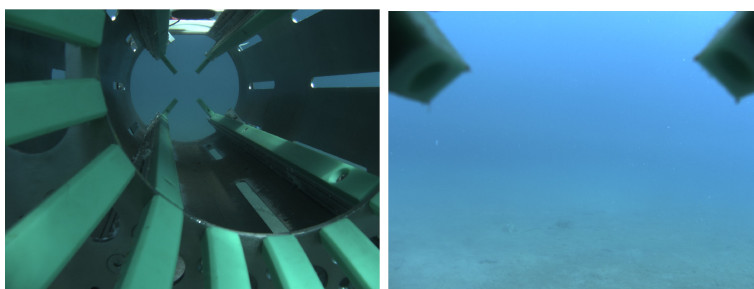

Figure 11: Location of the DS, Sant Feliu de Guíxols harbor. Image obtained from Google Maps. Note that for a better understanding, the DS is not in the correct scale.

Figure 12: On the left deployment of the DS at Sant Feliu de Guíxols harbor. On the right, DS inside the harbor of Sant Feliu de Guíxols.

(a) Sparus II at 11 meters from the DS.

(b) Sparus II at 5 meters from the DS.

(c) Sparus II at 2 meters from the DS.

(d) Sparus II inside the funnel of the DS.

(e) Sparus II completely inside the DS.

Figure 13: Frame sequence of the forward-looking camera of the Sparus II, developing an experimental autonomous docking in Sant Feliu de Guíxols.
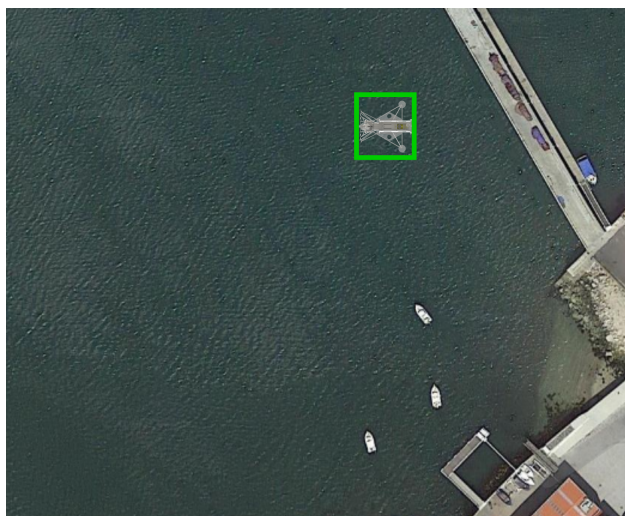
Figure 14: Location of the DS, Viana do Castelo harbor. Image obtained from Google Maps. Note that for a better understanding, the DS is not in the correct scale.
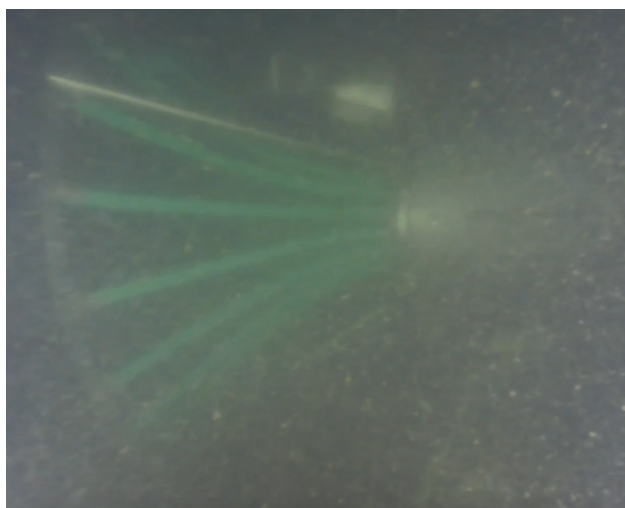

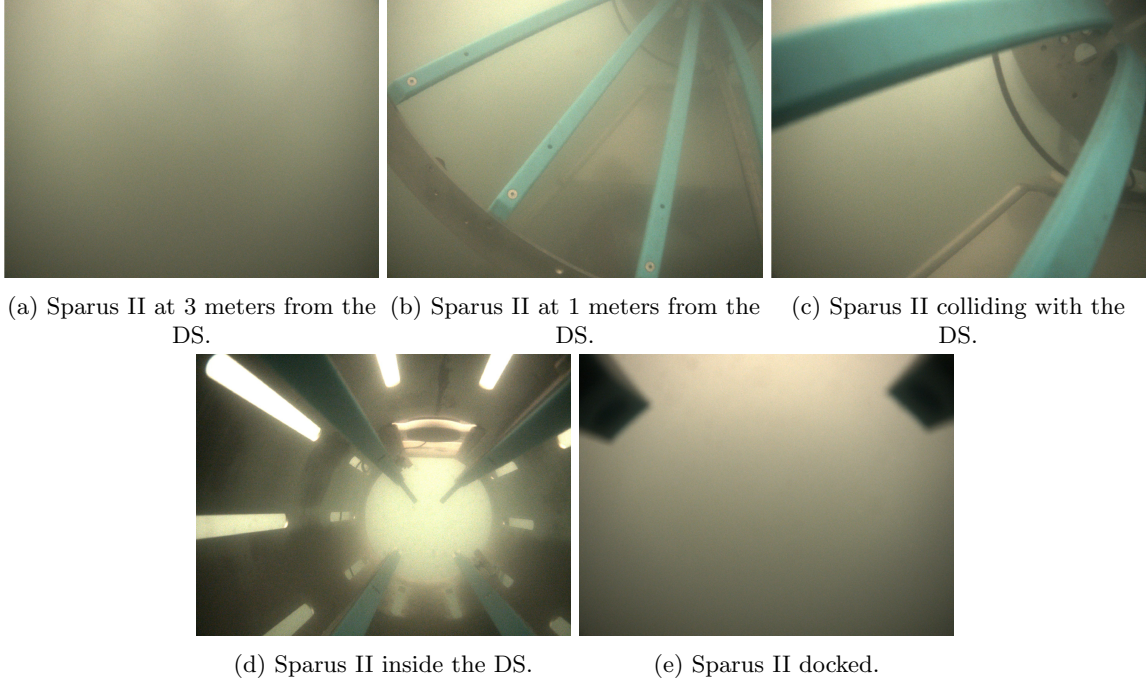Figure 15: DS inside the harbor of Viana do Castelo.

(a) Sparus II at 3 meters from the DS.

(b) Sparus II at 1 meters from the DS.

(c) Sparus II colliding with the DS.

(d) Sparus II inside the DS.

(e) Sparus II docked.

Figure 16: Frame sequence of the forward-looking camera of the Sparus II, developing an experimental autonomous docking in Viana do Castelo.

| Quality of the entrance into the DS: Sant Feliu							
Trial	#1	#2	#3	#4	#5	#6	#7
g	0.1192	0.8399	0.5263	0.9460	0.1172	0.9036	0.8252

Table 2: Analysis of the quality in the entrance of the AUV when it impacts to the DS (Esteba et al., 2021), for the last batch of tests developed in Sant Feliu de Guíxols.

entrance line. The surge velocity set-point (eq. (2)), modifies the surge speed to reduce the cross-track error either accelerating or reducing the speed (Fig. 17c and Fig. 17d). It is worth noting that the AUV desired velocity set to impact the DS ($\dot{x}_{ss}$) is 0.3 m/s, from which it is applied the correction (c), recall (2). Fig. 13 shows a sequence of images gathered with the frontal camera of Sparus II AUV, to illustrate the docking maneuver. With respect to the failed experiments, the first one, shown in Fig. 18a, was due to the absence of USBL fixes during the last 20 seconds of the mission, which caused a navigation drift. In this case, the cross-track error was driven to zero, but due to the navigation drift, the actual error was higher than the radius of the funnel entrance failing the docking. In the case of the second failure (Fig. 18b), the USBL updates make the robot aware it was located at the left of the DS beginning, therefore, a correction action. Unfortunately, too late to achieve the docking. The navigation system caused both failures, and therefore, the noise covariance matrix was adjusted to rise the influence of the USBL updates. Finally, a second batch of tests was launched, achieving seven consecutive autonomous docking maneuvers (see Fig. 19 and table 2), being considered as successful trial.
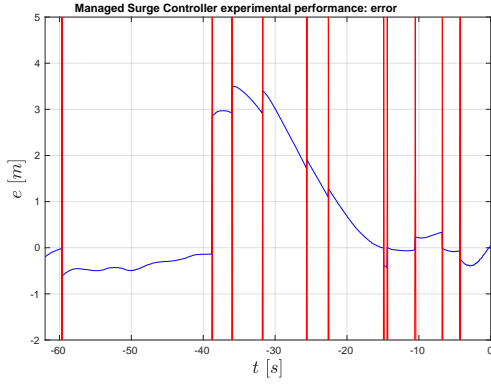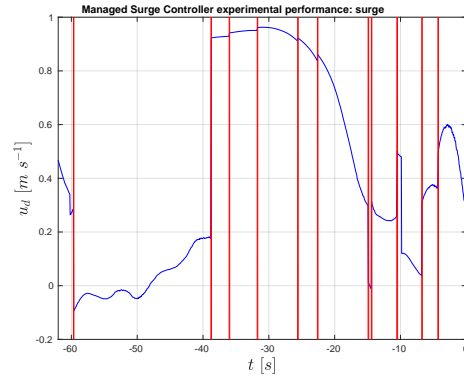
(a) Cross-track error against time representation, recall (1).
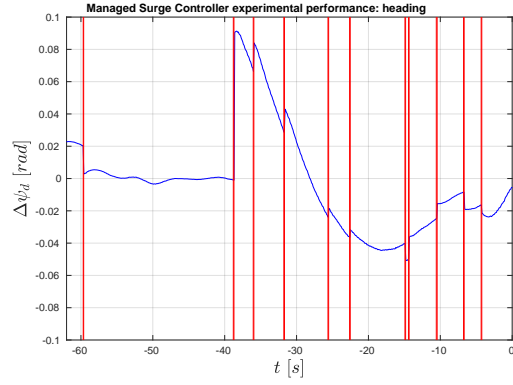
(b) Desired heading correction against time representation, following (3).
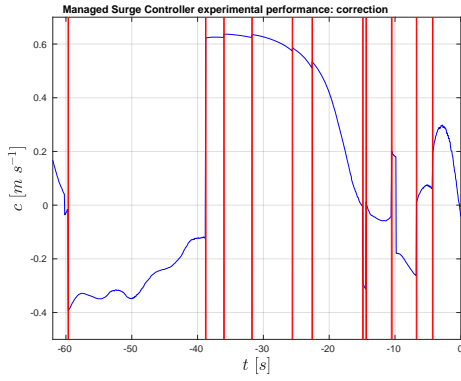
(c) Velocity correction against time representation, following (2).

(d) Desired surge velocity against time representation, following (2).

Figure 17: Representation of the performance of the MSC in one docking maneuver. Each vertical red line represents an update of the position of the AUV.

(a) Cross-track error against time representation of the first failed experiment, recall (1).
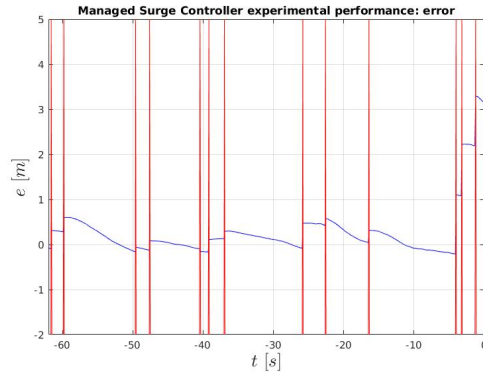
(b) Cross-track error against time representation of the second failed experiment, recall (1).

Figure 18: Representation of the error of the position of the AUV in the two failed maneuvers of the first test batch developed in Sant Feliu de Guíxols. Each vertical red line represents an update of the position of the AUV.

Figure 19: Representation of the seven autonomous docking maneuvers performed in Sant Feliu de Guíxols. Each color represents a different attempt. For the clarity of the image, the scale of the DS is not realistic, and a circle is represented at the beginning of each trajectory.
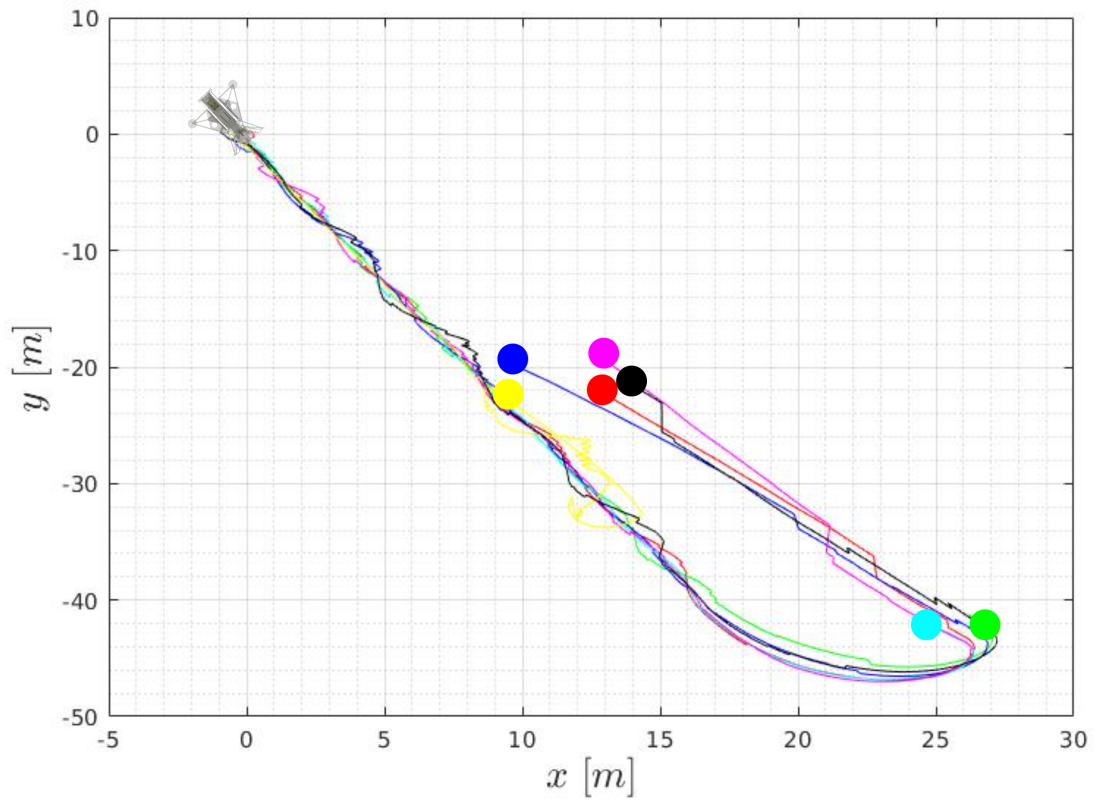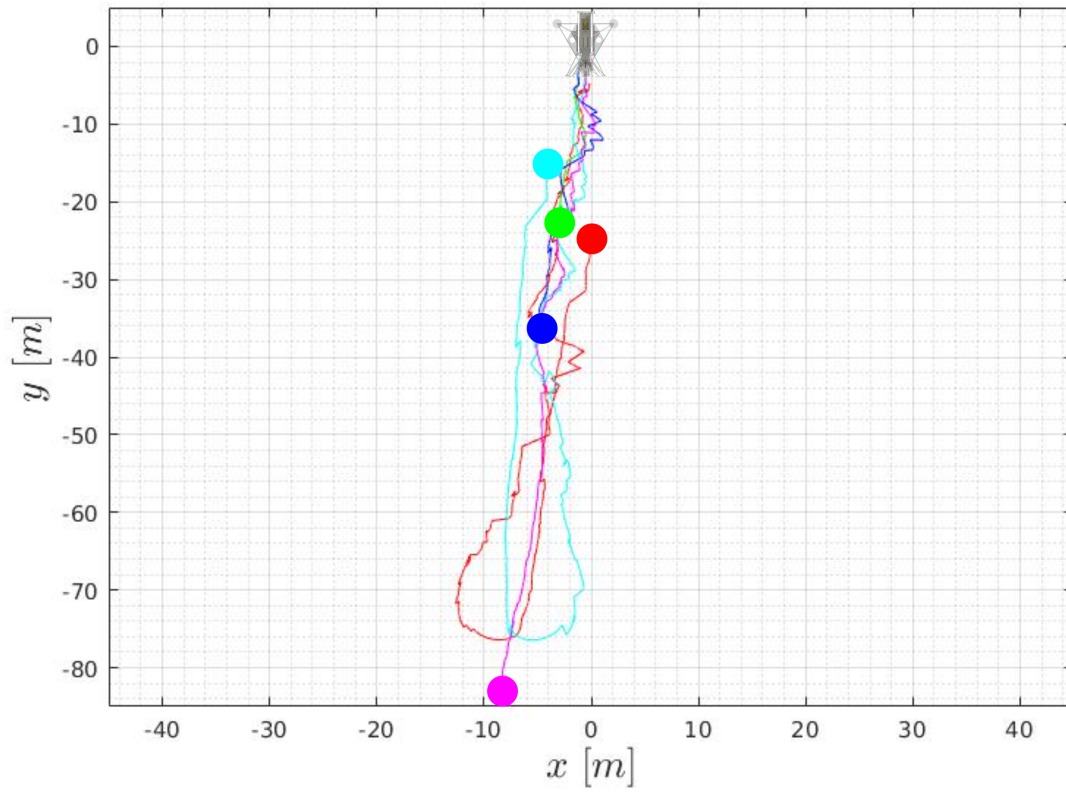
Figure 20: Representation of the seven autonomous docking maneuvers performed in Viana do Castelo. Each color represents a different attempt. For the clarity of the image, the scale of the DSis not realistic, and a circle is represented at the beginning of each trajectory.

Quality of the entrance into the DS: Viana					
Trial	#1	#2	#3	#4	#5
g	0.9513	0.4003	0.5765	0.7765	0.3881

Table 3: Analysis of the quality in the entrance of the AUV when it impacts to the DS (Esteba et al., 2021), for the last batch of tests developed in Viana do Castelo.

4.4 Results in Viana do Castello

Due to the water exchange between the river and the ocean, significant changes in salinity were observed depending on the area and depth. This affects the performance of the acoustic sensors, and degrades their performance, requiring further tuning of the navigation filter. Moreover, in this location, the time for testing was more restricted, due to the schedule of the experimental trials, the weather, and the vessel traffic. In these conditions, nine experiments were performed, the first four devoted to engineering trials and tuning, finalising with a batch of five consecutive docking maneuvers (table 3 and Fig. 20). Fig. 16 shows a camera frame sequence of a representative successful docking operation, where it can be appreciated the low visibility conditions of the area. As commented above, selecting a docking strategy based only on acoustic sensors feedback proved to be the right chose.

5 Conclusions

This paper presents a Long Term Deployment system for a non-holonomic AUV. The system is based on a motorized funnel-based docking station sensorized to be able to detect currents and self-align with them. The use of visual servoing methods to guide the docking has been explicitly avoided, to be able to operate in low visibility conditions. Therefore, the relative DS AUV navigation is tackled through an inverted USBL system conveniently integrated with the AUV navigation. The MSC algorithm, accounting for the ocean currents, has been employed to guide the docking. The system has been extensively tested in the field, using the Sparus II AUV, first in a harbor in Sant Feliu (Spain) and later on, in the ATLANTIS test center in Viana do Castelo (Portugal). In both cases with satisfactory results.

6 Future work

Future work will focus on testing the system under the influence of ocean currents. Unfortunately, this depends on the environmental conditions of the experimental site, as well as on the available logistics for the deployment, therefore, requiring detailed planning and preparation. Besides, we are conducting an energy consumption study and optimization of the DS, to guarantee long-term energetic autonomy.

Abbreviations

AUV Autonomous Underwater Vehicles

ROV Remotely Operated Vehicles

DS Docking Station

SDS Sparus Docking Station

MSC Managed Surge Controller

USBL Ultra Short BaseLine

EKF Extended Kalman Filter

AHRS Attitude and Heading Reference System

PID Proportional-integral-derivative controller

COLA2 Component orientated layer-based architecture for autonomy

ROS Robot Operating System

IMU Inertial Measurement Unit

DVL Doppler Velocity Log

GPS Global Positioning System

NED North, East, Down

LTD Long Term Deployment

LaRS Launch and Recovery System

UdG Universitat de Girona

DoF Degree of Freedom

COLA2 Component Orientated Layer-based Architecture for Autonomy

References

Allen, B., Austin, T., Forrester, N., Goldsborough, R., Kukulya, A., Packard, G., Purcell, M., and Stokey, R. (2006). Autonomous Docking Demonstrations with Enhanced REMUS Technology. *Oceans 2006*, pages 1–6.

Bellingham, J. G. (2016). Autonomous Underwater Vehicle Docking. In *Springer Handbook of Ocean Engineering*, chapter 16, pages 387–406. Springer, Cham.

Bluelogic. Bluelogic subsea docking station. `https://www.bluelogic.no/news-and-media/subsea-docking-station-sds-`. [Online; accessed 2023-01-31].

Blueprint Design Engineering Ltd. Blueprint subsea oculus imaging sonar. `https://www.blueprintsubsea.com/oculus/oculus-m-series`. [Online; accessed 2022-09-21].

Blueprint Design Engineering Ltd. Blueprint subsea seatrac x150 usbl beacon. `https://www.blueprintsubsea.com/seatrac/`. [Online; accessed 2022-09-21].

Carreras, M., Candela, C., Ribas, D., Mallios, A., Magí, L. L., Vidal, E., Palomeras, N., and Ridao, P. (2013). Sparus {II}, design of a lightweight hovering {AUV}. *Proceedings of the 5th international workshop on marine technology. Martech'13*, pages 152–155.

Carreras, M., Hernandez, J. D., Vidal, E., Palomeras, N., Ribas, D., and Ridao, P. (2018). Sparus II AUV - A Hovering Vehicle for Seabed Inspection. *IEEE Journal of Oceanic Engineering*, 43(2):344–355.

Circle, B. N. (2012). Underwater mobile docking of autonomous underwater vehicles. *OCEANS 2012 MTS/IEEE: Harnessing the Power of the Ocean*, pages 1–15.

Esteba, J., Cieslak, P., Palomeras, N., and Ridao, P. (2021). Docking of Non-holonomic AUVs in Presence of Ocean Currents: a Comparative Survey. *IEEE Access*.

Esteba, J., Cieslak, P., Palomeras, N., and Ridao, P. (2023). Managed Surge Controller : A Docking Algorithm for a Non-Holonomic AUV (Sparus II) in the Presence of Ocean Currents for a Funnel-Shaped Docking Station. *Sensors*, 23.

Feezor, M. D., Sorrell, F. Y., Blankinship, P. R., and Bellingham, J. G. (2001). Autonomous underwater vehicle homing/docking via electromagnetic guidance. *IEEE Journal of Oceanic Engineering*, 26(4):515–521.

Fletcher, B., Martin, S., Flores, G., Jones, A., Nguyen, A., Brown, M. H., and Moore, D. L. (2017). From the lab to the ocean: Characterizing the critical docking parameters for a free floating dock with a REMUS 600. *OCEANS 2017 - Anchorage*, 2017-Janua:1–7.

Hydromea. Luma x. `https://www.hydromea.com/underwater-wireless-communication`. [Online; accessed 2022-09-21].

INESC TEC. Atlantis test center promotional video. `https://youtu.be/7QW24hzu050`. [Online; accessed 2022-12-12].

Kawasaki, T., Noguchi, T., Fukasawa, T., Hayashi, S., Shibata, Y., Iimori, T., Okaya, N., Fukui, K., and Kinoshita, M. (2004). "Marine Bird," a new experimental AUV - Results of docking and electric power supply tests in sea trials. *Ocean '04 - MTS/IEEE Techno-Ocean '04: Bridges across the Oceans - Conference Proceedings*, 3:1738–1744.

Kukulya, A., Plueddemann, A., Austin, T., Stokey, R., Purcell, M., Allen, B., Littlefield, R., Freitag, L., Koski, P., Gallimore, E., Kemp, J., Newhall, K., and Pietro, J. (2010). Under-ice operations with a REMUS-100 AUV in the Arctic. *2010 IEEE/OES Autonomous Underwater Vehicles, AUV 2010*, pages 1–8.

LinkQuest Inc. Navquest micro dvl 600. `https://www.link-quest.com/html/intro_nq.htm`. [Online; accessed 2022-09-21].

Mbari. Mars system from mbari. `https://www.mbari.org/technology/monterey-accelerated-research-system-mars/`. [Online; accessed 2023-01-31].

McEwen, R. S., Hobson, B. W., Bellingham, J. G., and McBride, L. (2008). Docking control system for a 54-cm-diameter (21-in) AUV. *IEEE Journal of Oceanic Engineering*, 33(4):550–562.

Nicholson, J. and Healey, A. (2013). The Present State of Autonomous Underwater Vehicle (AUV) Applications and Technologies. *Marine Technology Society Journal*, 47(5):5–6.

Page, B. R. and Mahmoudian, N. (2020). Simulation-Driven Optimization of Underwater Docking Station Design. *IEEE Journal of Oceanic Engineering*, 45(2):404–413.

Palomeras, N., El-Fakdi, A., Carreras, M., and Ridao, P. (2012). COLA2: A control architecture for AUVs. *IEEE Journal of Oceanic Engineering*, 37(4):695–716.

Palomeras, N., Vallicrosa, G., Mallios, A., Bosch, J., Vidal, E., Hurtos, N., Carreras, M., and Ridao, P. (2018). AUV homing and docking for remote operations. *Ocean Engineering*, 154(May 2017):106–120.

Park, J. Y., huan Jun, B., mook Lee, P., and Oh, J. (2009). Experiments on vision guided docking of an autonomous underwater vehicle using one camera. *Ocean Engineering*, 36(1):48–61.

Park, J. Y., Jun, B. H., Lee, P. M., Oh, J. H., and Lim, Y. K. (2010). Underwater docking approach of an under-actuated AUV in the presence of constant ocean current. *IFAC Proceedings Volumes (IFAC-PapersOnline)*, 43(20):5–10.

Pinto, A. M., Marques, J. V., Campos, D. F., Abreu, N., Matos, A., Jussi, M., Berglund, R., Halme, J., Tikka, P., Formiga, J., Verrecchia, C., Langiano, S., Santos, C., Sa, N., Stoker, J. J., Calderoni, F., Govindaraj, S., But, A., Gale, L., Ribas, D., Hurtos, N., Vidal, E., Ridao, P., Chieslak, P., Palomeras, N., Barberis, S., and Aceto, L. (2021). ATLANTIS - The Atlantic Testing Platform for Maritime Robotics. *Oceans Conference Record (IEEE)*, 2021-Septe:1–5.

Quigley, M., Gerkey, B., Conley, K., Faust, J., Foote, T., Leibs, J., Berger, E., Wheeler, R., and Ng, A. (2009). ROS: an open-source Robot Operating System. *ICRA workshop on open source software*.

Raspberry Pi. Raspberry pi official website. `https://www.raspberrypi.com/products/raspberry-pi-3-model-a-plus/`. [Online; accessed 2023-01-31].

Sarda, E. I. and Dhanak, M. R. (2019). Launch and Recovery of an Autonomous Underwater Vehicle from a Station-Keeping Unmanned Surface Vehicle. *IEEE Journal of Oceanic Engineering*, 44(2):290–299.

Singh, H., Bellingham, J. G., Hover, F., Lerner, S., Moran, B. A., Von Der Heydt, K., and Yoerger, D. (2001). Docking for an autonomous ocean sampling network. *IEEE Journal of Oceanic Engineering*, 26(4):498–514.

Smith, R., Self, M., and Cheeseman, P. (1990). *Estimating Uncertain Spatial Relationships in Robotics*, pages 167–193. Springer New York, New York, NY.

Stokey, R., Allen, B., Austin, T., Goldsborough, R., Forrester, N., Purcell, M., and Von Alt, C. (2001). Enabling technologies for REMUS docking: An integral component of an autonomous ocean-sampling network. *IEEE Journal of Oceanic Engineering*, 26(4):487–497.

Stokey, R., Purcell, M., Forrester, N., Austin, T., Goldsborough, R., Allen, B., and von Alt, C. (1997). Docking system for REMUS, an autonomous underwater vehicle. *Oceans Conference Record (IEEE)*, 2:1132–1136.

Universitat de Girona. Opthirov research project official website. `https://optihrov.udg.edu/`. [Online; accessed 2022-12-21].

Universitat de Girona. Plome research project official website. `https://plomeproject.es/`. [Online; accessed 2022-12-21].

Whitcomb, L. L. (2000). Underwater robotics: out of the research laboratory and into the field. *Proceedings - IEEE International Conference on Robotics and Automation*, 1:709–716.

Yazdani, A. M., Sammut, K., Yakimenko, O., and Lammas, A. (2020). A survey of underwater docking guidance systems. *Robotics and Autonomous Systems*, 124.

Zhang, T., Li, D., and Yang, C. (2017). Study on impact process of AUV underwater docking with a cone-shaped dock. *Ocean Engineering*, 130(December 2016):176–187.